International Journal of GEOMATE, June 2019, Vol.16, Issue 58, pp.97 - 103
Geotec., Const. Mat. & Env., DOI: https://doi.org/10.21660/2019.58.8171
ISSN: 2186-2982 (Print), 2186-2990 (Online), Japan

VOLUME CHANGE BEHAVIOR OF SEA WATER EXPOSED COAL ASH USING HYPERBOLIC MODEL

*Erica Elice S. Uy[1], Mary Ann Q. Adajar[1] and Jonathan R. Dungca[1]

[1]Department of Civil Engineering, De La Salle University, Philippines

*Corresponding Author, Received: 27 Oct. 2018, Revised: 29 Dec. 2018, Accepted: 12 Jan. 2019

ABSTRACT: The Philippines greatly relies on coal-fired power plants as a source of electricity. These power plants produce a by-product or waste material called coal ash. In recent years, the country has been experiencing continuous urbanization. As a result, there is an increase in the demand for electricity consumption. This can also result in an increase in production of coal ash. There are several studies that suggest the potential of coal ash as a construction material. In this study, the coal ash was exposed to seawater. In order to investigate the potential of coal ash as a construction material to structures that will be exposed to the sea. Consolidated drained triaxial test was performed considering the following level of exposure namely, no exposure, immediate exposure, and prolonged exposure. A hyperbolic model was used to model the stress-dependent volume change behavior of the material towards sea water. In the model, the Poisson's ratio parameters were determined. The tangent value of Poisson's ratio and its relationship with the applied stressed was evaluated.

Keywords: Bottom Ash, Volume Change, Poisson's Ratio, Hyperbolic Model

1. INTRODUCTION

Coal-fired power plants remain to be a dominant producer of energy in the Philippines. According to BMI research, the share of coal in energy production is continuously increasing. The predicted increase in 2017 was only up to 50 percent. However, in 2018, the predicted increase will be more than 50 percent and this trend is expected to occur until the year 2027 [1]. About 75% of the coal supply is imported from Indonesia and Australia [1]. The importation will be lessened since there is an increase in production from a power plant at the Visayas and a newly operated power plant at Mindanao. Semirara Mining and Power Corporation are one of the leading coal producers in the Visayas aims to increase its production. Target production of 16 million metric tons in two or three years is the goal of the company in order to meet the demand of the consumers [2]. The continuous increase in demand can result in more production of waste materials. These waste materials or by-product are called coal ash. These are stored in ash ponds. The increase in demand can cause a shortage of storage facilities. This might lead to the improper way of disposal due to the lack of available ash ponds. To avoid this, several types of research were conducted to determine the potential of coal ash as a construction material. There are many types of coal ash by-products or coal combustion by-products (CCB). The most frequently studied in researches are fly ash and bottom ash [3]-[8]. These waste materials were utilized as a road base construction material as a partial substitute for conventional materials [3]-[6]. The performance of these by-products to improve the hydraulic conductivity characteristics of the road base was explored. Blending the by-products had an effect on the hydraulic conductivity of soils. A percentage substitute ranging from 40% to 60% of bottom ash resulted to the highest vertical hydraulic conductivity [3]. The use of bottom ash in highway embankments, subgrades and subbases were also investigated. Based on the results, the by-product was able to satisfy the material specification for a subgrade and subbase [4]. In another study, the performance of coal ash as a construction material for land reclamation near the sea was evaluated. Coal ash was exposed to sea water to simulate the actual conditions of the reclamation site. Modified Cam Clay model was incorporated in the study. The model resulted in determining the maximum deviator stress and maximum mean normal effective stress of coal ash at its elastic state. The maximum deviator stress has a value of 600 kPa while the maximum mean normal effective stress is 500 kPa. Based on their findings, bottom ash has the potential to be used as a construction material for a reclamation project [7]. The potential of coal ash as a road embankment exposed to seawater was also investigated. A Hyperbolic model was used in the study to establish the parameters and understand the material's stress-strain response. The prediction showed an increase in the ultimate deviator stress the by-product can accommodate [8]. Although several studies showed the potential of coal ash as a construction material, its volume change behavior with regards to seawater exposure needs to be further understood. This behavior needs to be understood due to the growing population in major cities such as Manila and Cebu City. Most of these cities experiences congestion which resulted to constructing additional infrastructures at bodies of water. It is therefore the objective of this study to understand the volume change behavior of coal ash exposed to seawater. A hyperbolic model was used to model and predict the volume change behavior of coal ash towards the sea water. Furthermore, hyperbolic parameters with respect to the Poisson's ratio and bulk modulus were also obtained. Seawater exposure was performed in three levels of exposure namely, no exposure (S1), immediate exposure (S2) and prolonged exposure (S3). Consolidated drained triaxial test was performed.

2. INDEX PROPERTIES OF BOTTOM ASH

The bottom ash used in the study was obtained from a power plant in the central Philippines. The index properties of bottom ash are tabulated in Table 1. These were established based on the procedures specified by the American Society for Testing Materials. Based on the results, the by-product was classified as silty sand (SM) with no plasticity. It also contains a sufficient amount of sand particles with fines content. The result of specific gravity as compared to other studies. A range of 1.899 to 1.903 was established [9]. It can be seen that the specific gravity determined had a larger value. It is rather close to the typical values for silty sand which is 2.6 to 2.9 [10]. The location where the tested coal ash was different from the coal ash tested from the other study. This could have contributed to the difference in the result of the tested coal ash.

Table 1. Index properties

Index Property	
Specific gravity(Gs)	2.25
Liquid limit(LL)	0.00%
Plastic limt (PL)	0.00%
Maximum void ratio (e_{max})	0.94
Minimum void ratio (e_{min})	0.85
Maximum dry unit weight(γ_{dmax})	13.94 kN/m^3
Optimum water content (ω_{opt})	15.85%
USCS	SM
%Gravel	0.86
%Sand	50.44
%Fines	48.70

Table 2 Chemical composition of seawater

Compound	Concentration,g/L
NaCl	24.53
MgCl	5.2
NaSO	4.09
CaCl	1.16
KCl	0.695
NaHCO	0.201
KBr	0.101
HBO	0.027
SrCl	0.025
NaF	0.003
Ba(NO	9.94E-05
Mn(NO	3.40E-05
Cu(NO	3.08E-05
Zn(NO	9.60E-06
Pb(NO	6.60E-06
AgNO	4.90E-07

3. EXPERIMENTAL PROGRAM

3.1 Sea water Preparation and Exposure Levels

The Standard Practice for the Preparation of Substitute Ocean Water (ASTM D 1141 – 98) was used to artificially prepare the sea water. Actual sea water was not used due to environmental concerns. The chemical compositions used for the mixing of artificial seawater are tabulated in Table 2. Seawater exposure level was divided into three namely, no exposure (S1), immediate exposure (S2) and prolonged exposure (S3). In a no exposure level, distilled water was used in the sample preparation and in the experiment. The immediate exposure, on the other hand, had sea water exposure during the experiment. Lastly, the prolonged exposure level is where seawater was used in the sample preparation and in the experiment.

3.2 Cyclic Triaxial Test

Coal ash was prepared by moist tamping. The relative compaction was used as the parameter to reach the initial target condition. This parameter was used in order to simulate actual site conditions. The maximum dry density was used as the reference to reach the desired relative compaction. A 95% relative compaction was the initial target condition and this value was also the desired in-situ condition. For the sample preparation of S1 and S2, the amount of distilled water mixed with coal ash was referenced with the optimum moisture content. Similarly, for the sample preparation of S3, the value of optimum moisture content served as the reference parameter in order to determine the amount of seawater to be mixed with coal ash. The samples for all levels were soaked for 16 hours as stipulated in the ASTM provisions.

3.3 Consolidated Drained Test

British Standard (BS) 1377-8: 1990 was the standard applied in performing the Consolidated Drained Test. Based on the standard, there are three stages in the experiment namely, saturation, consolidation and shear. The saturation stage is where additional water is added to the sample. In the study especially in S3, salt water was added in this stage. In order to ensure that a fully saturated condition was achieved a B-value or the ratio of the change in pore water pressure and confining pressure was checked. This parameter must have a value greater than 0.95. In the consolidation stage, the confining pressures (σ_3) used are 50 kPa, 100 kPa, and 200 kPa. In S2 and S3 the sea water was used to confine the sample during the consolidation and shearing stage. For the shearing stage, the rate of loading of 0.05 mm/min was implemented. This rate was used in order to facilitate the proper dissipation of pore water pressure. The shearing stage lasted for a minimum of 4 hours to a maximum of 7 hours due to the slow rate. A total of 18 samples were tested for this study.

4. HYPERBOLIC MODEL

The Hyperbolic model is based on the hyperbolic stress-strain relationship [11]. It is an incremental stress-dependent model which is based on the incrementally nonlinear elastic behavior. The model can represent the nonlinear behavior of the volume change through hyperbolas. Poisson's ratio can be determined from the model through the analysis of the volume changes in a triaxial test. This parameter is computed by determining the radial strains as shown [12]:

$$\varepsilon_r = \frac{1}{2}(\varepsilon_v - \varepsilon_a) \tag{1}$$

where ε_v = volumetric strain; ε_a = axial strain.

The variation of ε_a with ε_r is when plotted can result in the following hyperbolic equation [12]:

$$\varepsilon_a = \frac{-\varepsilon_r}{v_i - d\varepsilon_r} \tag{2}$$

When ε_r is normalized with ε_a, the equation can be rewritten as shown in Eq.3. Typical results are shown in Fig.1. This equation can determine the value of the Poisson's ratio or initial Poisson's ratio [12].

$$-\frac{\varepsilon_r}{\varepsilon_a} = v_i - d\varepsilon_r \tag{3}$$

where v_i = initial Poisson's ratio (at zero strain) or the y-intercept of the plot; d = parameter representing the change in the value of Poisson's ratio with radial strain or the slope of the plot.

The equation of each plot in Fig. 1 is expressed as:

$$-\frac{\varepsilon_r}{\varepsilon_a} = \mathbf{0.4811 - 1.0316}\boldsymbol{\varepsilon_r} \tag{4}$$

$$-\frac{\varepsilon_r}{\varepsilon_a} = \mathbf{0.4406 - 0.5477}\boldsymbol{\varepsilon_r} \tag{5}$$

$$-\frac{\varepsilon_r}{\varepsilon_a} = \mathbf{0.4980 - 2.0892}\boldsymbol{\varepsilon_r} \tag{6}$$

where Eqn 4 is the plot for 50kPa cell pressure; Eqn 5 is the plot for 100kPa cell pressure; Eqn 6 is the plot for 200kPa cell pressure.

Poisson's ratio was found to be affected by the change in confining pressure. The volume change behavior, therefore, can be represented through varying Poisson's ratio with confining pressure as shown in Eqn. 7 [12].

$$v_i = G - F log_{10}\left(\frac{\sigma_3}{P_a}\right) \tag{7}$$

where G = the value of v_i at a confining pressure of one atmosphere; F = the reduction in v_i for a ten-fold increase in confining pressure.

The parameters presented in Eqn. 7 can be determined by plotting v_i against the ratio of the confining pressure and atmospheric pressure. Typical results are shown in Fig. 2.

The instantaneous slope, tangent value of Poisson's ratio (v_t), of the variation of ε_a with ε_r can also be related to the changes in the stress of the sample. It can be defined by the following expression [12]:

$$v_t = \frac{G - F log\left(\frac{\sigma_3}{P_a}\right)}{\left[1 - \frac{d(\sigma_1 - \sigma_3)}{KP_a\left(\frac{\sigma_3}{P_a}\right)^n\left[1 - \frac{R_f(\sigma_1-\sigma_3)(1-sin\varphi)}{2ccos\varphi + 2\sigma_3 sin\varphi}\right]}\right]^2} \tag{8}$$

where K = primary loading modulus; n = exponent number; C = cohesion; R_f = failure ratio; φ = angle of internal friction; Pa = atmospheric pressure (Pa = 101.325 kPa).

Bulk modulus was replaced by Poisson's ratio in analyzing the volume change behavior of the soil [13]. This parameter is independent of changes in deviator stress. However, it still varies with confining pressure. Bulk modulus, therefore, can provide approximations that are reasonable to the behavior of changes in volume. Moreover, assuming that the bulk modulus is independent of the changes in deviator stress can appropriately characterize the response of the soil with respect to the variations in the mean stresses. Based on the theory of elasticity, bulk modulus can be defined by the following expression:

$$B = \frac{\Delta\sigma_1+\Delta\sigma_2+\Delta\sigma_3}{3\varepsilon_v} \quad (9)$$

where B = bulk modulus; $\Delta\sigma_1$, $\Delta\sigma_2$ and $\Delta\sigma_3$ = changes in the values of the principal stresses; $\Delta\varepsilon_v$ = change in volumetric strain.

In a conventional triaxial test, Eqn.9 can be re-written to Eqn.10 since the confining pressure is maintained at a constant value while the deviator stress is being increased.

$$B = \frac{\sigma_1-\sigma_3}{3\varepsilon_v} \quad (10)$$

The bulk modulus can be computed with respect to the variation of confining pressure in relation to the hyperbolic model. As the confining pressure increases the bulk modulus also increases [13]. The bulk modulus, therefore, can be approximated by this equation:

$$B = K_b P_a \left(\frac{\sigma_3}{P_a}\right)^m \quad (11)$$

where K_b = bulk modulus number; m = bulk modulus exponent.

The parameters K_b and m are determined by plotting the normalized bulk modulus against confining pressure on a logarithmic scale. Typical results are shown in Fig. 3. Parameter m is the slope of the plot while parameter K_b is the y-intercept.

5. VOLUME CHANGE BEHAVIOR OF COAL ASH

The hyperbolic parameters with respect to the volume change behavior of the coal ash exposed to seawater were determined. The results related to Poisson's ratio are tabulated in Tables 3-5.

Table 3 Hyperbolic Parameters for S1

σ_3 kPa	d	v	G	F	v_t
50	1.0316	0.4811			0.1379
100	0.5477	0.4406	0.4524	0.0181	0.0032
200	2.0892	0.4980			0.1320

Table 4 Hyperbolic Parameters for S2

σ_3 kPa	d	v	G	F	v_t
50	1.1094	0.5217			0.0085
100	0.1292	0.5018	0.5187	0.0072	1.5407
200	0.6955	0.5078			0.2294

Table 5 Hyperbolic Parameters for S3

σ_3 kPa	d	v	G	F	v_t
50	0.2857	0.5045			0.7956
100	0.1582	0.5018	0.4960	0.0085	0.6776
200	2.2760	0.5136			0.0096

The results from the different level of seawater exposure were compared. Based on the results, it was observed that at 100 kPa all the parameters are smaller than the results from 50 and 200 kPa except the trend for the tangent value of Poisson's ratio. The tangent value of Poisson's ratio has no distinct trend. The results were greatly affected by K, n, R_f C, and the angle of internal friction. The parameters K, n and R_f used are tabulated in Table 7. It can be observed that K and n for S1 and S2 are the same while a smaller value was observed for S3. The angle of internal friction for S1, S2 and S3 are 33.77˚, 27.03˚ and 33.91˚, respectively [8]. The cohesion for S1, S2 and S3 are 28.56 kPa, 49.91 kPa and 15.43 kPa, respectively [8]. The angle of internal friction for S2 exposure was smaller compared to the other samples. On the other hand, its cohesion is larger. These parameters affected the results of the tangent value of Poisson's ratio.

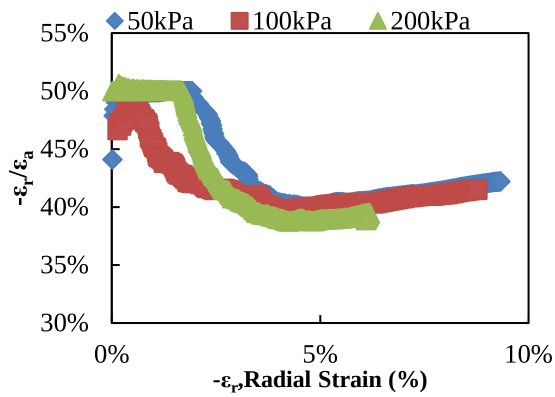

Fig.1 Hyperbolic axial strain-radial strain curve.

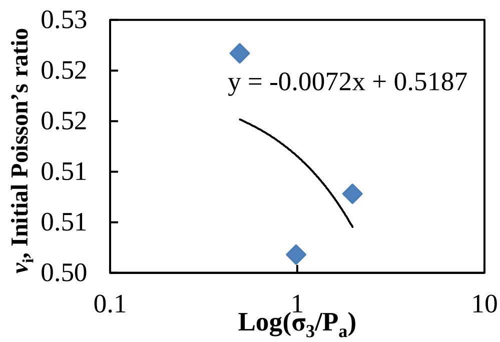

Fig.2 Variation of v_i with σ_3.

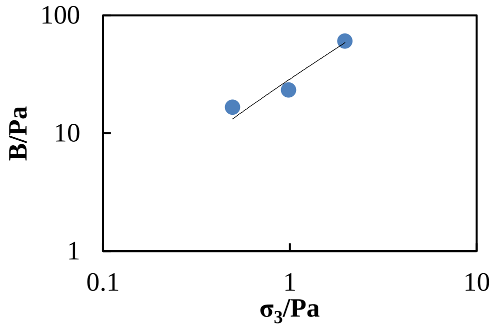

Fig. 3 Variation of bulk modulus with σ_3.

The hyperbolic parameters with respect to the bulk modulus were also obtained. Results are tabulated in Table 6. The bulk modulus was determined with respect to a constant m and K_b and increasing confining pressure. It can be seen that as the confining pressure was increased the bulk modulus also increases. The bulk modulus can better approximate the volumetric response of the soil. Therefore, it was used to predict the volume change of each seawater exposure levels. The typical results of S1 and S2 are shown in Figs.4-6 and Figs7-9, respectively. The typical results for S3 are similar to S2. The predicted results for S1 at 50 kPa coincided with the experimental results but this was towards the end of the plot. For 100 kPa, only a part in the plot coincided with the predicted results. For 200 kPa, the predicted results only followed the trend of the experimental results. As a whole, the predicted results for S1 was larger than the experimental results. For the results of S2, the predicted results for 50 kPa and 200 kPa had a similar trend. The predicted results coincided towards the end of the plot. The 100 kPa predicted results, on the other hand, was larger than the experimental data.

Table 6 Hyperbolic Parameters with respect to B

	m	K_b	σ_3, kPa	B, kPa	
S1			50	1,534.8211	
	0.9303	29.2216	100	2,924.8450	
			200	5,573.7558	
S2			50	2,936.0899	
	0.7295	48.5097	100	4,868.2738	
			200	8,071.9906	
S3			50	8,999.2595	
	1.3238	226.22973	100	22,526.7661	
			200	56,388.5495	

Based on the results, the hyperbolic model was not able to fully predict the volume change behavior of the coal ash. The parameters established were affected by the behavior of volume change data of each sea water level exposure. For all samples tested it was observed that the volume change behavior did not reach a stable value. Especially for the samples exposed to seawater. The pore water pressure was not able to properly dissipate.

Table 7 Hyperbolic stress-strain parameters [8].

	K	N	σ_3, kPa	R_f
S1	5.9900	1.34	50	0.9998
			100	0.9324
			200	0.5335
S2	5.9900	1.34	50	0.9051
			100	0.9282
			200	0.8309
S3	4.6600	0.22	50	0.9946
			100	0.9192
			200	0.8207

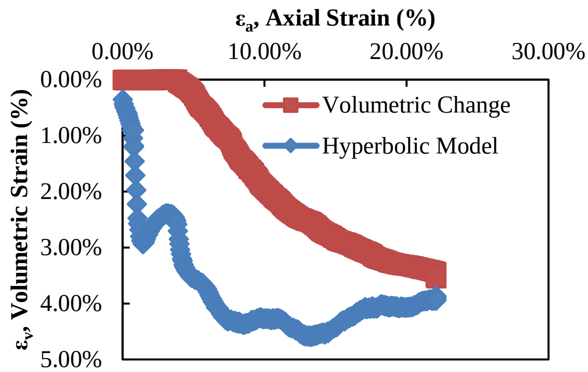

Fig.4 Results for S1 at 50kPa.

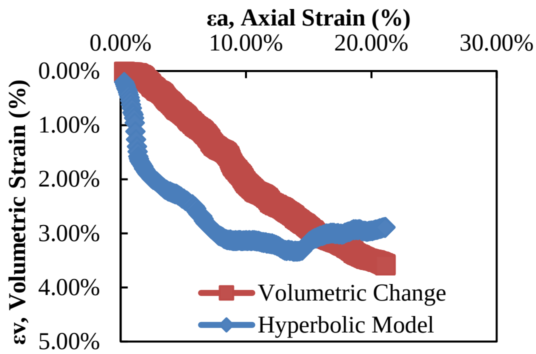

Fig.5 Results for S1 at 100kPa.

Seawater greatly affected the drainage condition during the experiment. For the results of S2 and S3, they were affected by the consistency of the relative compaction. The mixture of seawater with respect to the coal ash was the main factor that affected the relative compaction. The established hyperbolic parameters were observed to be highly affected by the drainage conditions and the reaction of sea water when mixed to the bottom ash.

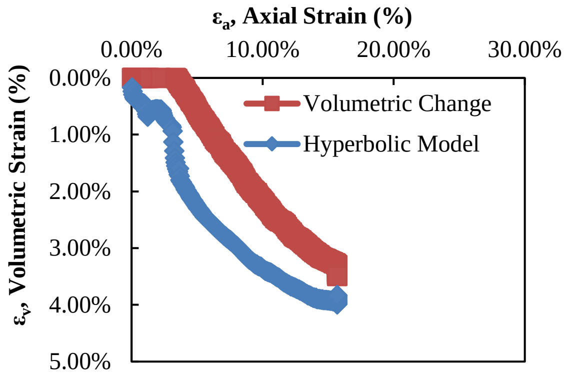

Fig.6 Results for S1 at 200kPa.

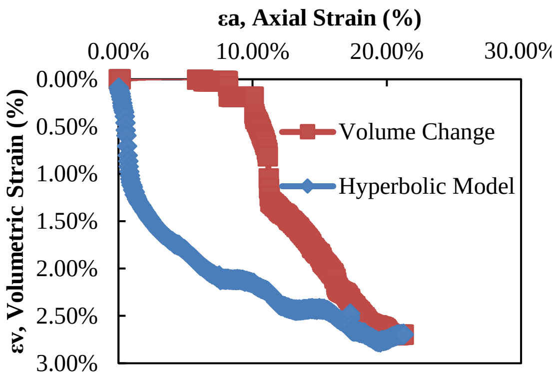

Fig.7 Results for S2 at 50kPa.

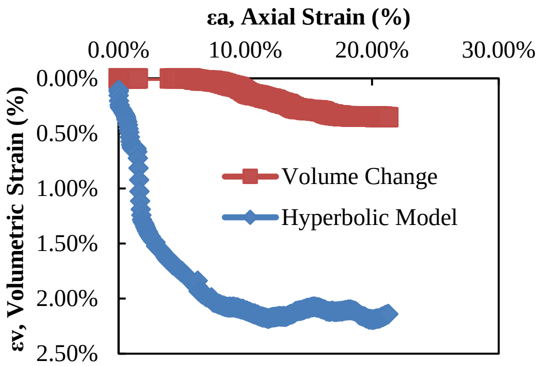

Fig.8 Results for S2 at 100kPa.

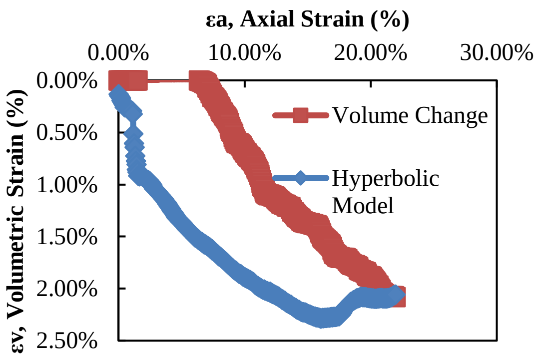

Fig.9 Results for S2 at 200kPa.

6. CONCLUSIONS

The hyperbolic model was implemented to investigate on the volume change behavior of the coal ash exposed to seawater. Based on the results, the parameter representing the change in the value of Poisson's ratio with radial strain (d), the value of ν_i at a confining pressure of one atmosphere (G) and the reduction in ν_i for a ten-fold increase in confining pressure (F) are affected by the amount of confining pressure. The tangent value of Poisson's ratio, on the other hand, is affected by the primary loading modulus (K), exponent number (n), failure ratio (R_f), cohesion (C) and the angle of internal friction. For the prediction of the volume change behavior of the hyperbolic model, it was observed that the model was not able to fully predict the volume change behavior of the coal ash. The parameters obtained were observed to be affected by the drainage conditions and the reaction of sea water when mixed to the bottom ash. It is recommended to perform more experiments having a wider range of confining pressure. A different loading rate should also be considered. This is to improve the parameter determination with respect to the hyperbolic model.

7. ACKNOWLEDGMENTS

The researcher would like to express her deep gratitude towards Dr. Mary Ann Q. Adajar, Dr. Jonathan Dungca and De La Salle University for their support.

8. REFERENCES

[1] The Inquirer. "Coal Remain Dominant In Philippine Energy Mix", http://business.inquirer.net/243956/coal-remain-dominant-ph-energy-mix, 2018.

[2] Department of Energy. "Coal Top 55 Philippine Power Mix 2027", https://www.doe.gov.ph/energist/coal-top-55-ph-power-mix-2027, 2018

[3] Yoon, S., Ph, D., Balunaini, U., Yildirim, I. Z., Prezzi, M., and Siddiki, N. Z., "Construction of An Embankment with A Fly And Bottom Ash Mixture : Field Performance Study", Journal of Materials in Civil Engineering, Vol.21, 2009, pp.271–278

[4] Dungca, J. R. and Jao, J. A. L., "Strength and Permeability Characteristics of Road Base Materials Blended With Fly Ash and Bottom Ash", International Journal of GEOMATE, Vol.12, Issue 31, 2017, pp. 9-15.

[5] Dungca, J. R., Galupino, J.G., Alday, J.C., Baretto, M.A.F., Bauzon, K. G. and Tolentino,

A. N., "Hydraulic Conductivity Characteristics of Road Base Materials Blended with Fly Ash And Bottom Ash", International Journal of GEOMATE, Vol.14, Issue 44, 2018, pp.121-127.
[6] Huang, W. H., "The Use of Bottom Ash in Highway Embankments, Subgrades and Subbases", Retrieved from docs.lib.purdue.edu/cgi/viewcontent.cgi?article=1782&context=jtrp. 1990.
[7] Uy, E. E. S. and Dungca, J. R., "Constitutive Modeling of Coal Ash using Modified Cam Clay Model. International Journal of GEOMATE, Vol. 12, Issue 31, 2017, pp.88-94.
[8] Uy, E. E. S. and Dungca, J. R., "Hyperbolic Model Parameters of Philippine Coal Ash", International Journal of GEOMATE, Vol. 15, Issue 47, 2018, pp.95-102.
[9] Antonio, O. V. M., and Zarco, M. A. H., "Engineering Properties of Calaca Batangas Bottom Ash", Vol. 28, Issue 1, 2007, pp.37–56.
[10] Das, B. & Sobhan, K., "Principles of Geotechnical Engineering", Sixth Edition, United States: Chris Carson, 2014
[11] Stark, T. D., Ebeling, R. M. & Vettel, J. J., "Hyperbolic stress-strain parameters for silts. Journal of Geotechnical Engineering", Vol.120, Issue 2, 1992, pp.420-441.
[12] Duncan, J. and Wong, K., "Hyperbolic Stress-Strain Parameters for Nonlinear Finite Element Analyses of Stress and Movements in Soil Masses", Report No TE-74-3, University of California, Berkeley, California, 1974.
[13] Duncan, J. and Wong, K., "Strength, Stress-strain and Bulk Modulus Parameters for Finite Element Analysis of Stresses and Movements in Soil Masses", Report No. UCB/GT/80-01, University of California, Berkeley, California, 1980.

Copyright © Int. J. of GEOMATE. All rights reserved, including the making of copies unless permission is obtained from the copyright proprietors.